NASA TM-84578

NASA-TM-84578 19830007090

NASA Technical Memorandum 84578

STRESS ANALYSIS OF ADVANCED ATTACK HELICOPTER COMPOSITE MAIN ROTOR BLADE ROOT END LUG

Donald J. Baker

December 1982

NASA
National Aeronautics and
Space Administration

Langley Research Center
Hampton, Virginia 23665

STRESS ANALYSIS OF ADVANCED ATTACK HELICOPTER COMPOSITE MAIN ROTOR BLADE ROOT END LUG

Donald J. Baker
Structures Laboratory
U. S. Army Research and Technology
Laboratories (AVRADCOM)
Langley Research Center
Hampton, VA

SUMMARY

Stress analysis of the Advanced Attack Helicopter (AAH) composite main rotor blade root end lug is described. The stress concentration factor determined from a finite element analysis is compared to an empirical value used in the lug design. The analysis and test data indicate that the stress concentration is primarily a function of configuration and independent of the range of material properties typical of Kevlar-49/Epoxy and Glass/Epoxy.

INTRODUCTION

Composite rotor blades offer a number of advantages such as reduced manufacturing cost and increased life when compared to metal blades. To capitalize on these advantages, a Manufacturing Methods and Technology (MM&T) program was initiated to design, fabricate and test a composite main rotor blade for The Advanced Attack Helicopter (AAH). Two designs have evolved from this MM&T program. The first design (A) is an all Kevlar-49[1]/APCO 2434[2] epoxy blade as shown in figure 1a. The second design (B) is similar to design (A) except for Graphite/epoxy doublers at each lug surface in lieu of the Kevlar-49/epoxy skin. The second design was required because testing of the design (A) root end element produced early fatigue failures in the attachment lugs (figure 1b). The Structures Laboratory-USARTL was requested by

---

[1]Registered Trademark of Dupont Co.

[2]Manufactured by Applied Plastics Corp.

N83-15361

the Directorate for Systems Engineering and Development (AVRADCOM) to perform a finite element analysis of the lug. Stress concentration factors for the lug have been computed for each design using a finite element analysis. Radial stress in the lug adjacent to the attachment pin has also been calculated. Results of the finite element analysis are compared to results based on empirical methods used in the initial design and analysis.

Certain commercial materials are identified in this paper in order to specify adequately which materials were investigated in the research effort. In no case does such identification imply that the materials are necessarily the only ones or the best ones available for the purpose. In many cases equivalent materials are available and would probably produce equivalent results.

ROTOR BLADE DESCRIPTION

Primary load carrying members for the all-composite rotor blade are unidirectional Kevlar-49/epoxy spar caps (see figure 2). Each of the upper and lower spar caps has two bundles that are continuous from the blade tip and are wrapped around steel bushings where the blade attaches to the hub. These unidirectional spar caps are laid on rectangular [±45°] Kevlar-49 fabric/epoxy tubes that form the center or core of the blade as shown in figures 2 and 3. The assembly is overwrapped with [±45°] Kevlar-49/epoxy skins of varying thickness. Spar cross sectional areas and skin thickness are given in Table 1 for blade stations near the root end. The Kevlar-49/epoxy skins between the lug end and station 42.5 in Design (A) are replaced with a Graphite/epoxy doubler for Design (B).

LUG ANALYSIS

The lug analysis was performed using two finite element models. The area between the root end and station 51.5 was modeled using 2-D combined membrane-bending elements. The local area around the lug was also modeled with 3-D elastic solid elements.

2-D Analysis

The 2-D analysis of the lug was performed using SPAR, Level 14, finite element code, reference (1). Quadrilateral and triangular elements with combined membrane and bending stiffness were used to obtain the stress distribution. The 2-D finite element model used in this analysis is shown in figure 4. The blade root-end is symmetric about the X-Y and X-Z plans and has a symmetrically applied load. Therefore only one fourth of the root-end was modeled for the analysis. The airfoil contour was modeled by following the centerline of the spar caps (figure 2) with the elements. This results in the out of plane views shown in figure 4 View A-A & View B-B. Properties for each material were obtained[3] and are given in Table 2. Spar cap areas and skin thicknesses used to define the finite elements are listed in Table 1.

The boundary conditions which bound the actual condition have been analyzed. Condition I has the root attachment pin fixed in the x-direction and free to move in the y-direction. Condition II has the root attachment pin fixed in both directions.

An axial load representing a centrifugal force of 66.7 kN was applied at Blade Station 51.5 by prescribing a uniform axial displacement. The internal stress distribution was determined and then the applied load required to produce failure was calculated with a linear analysis.

3-D Analysis

The 2-D analysis cannot accurately predict stress distribution through the lug thickness, or the interaction of pin bending with the lug. The structure was modeled using the EISI/EAL finite element code (reference 2) which is a newer version of SPAR and has improved algorithms for 3-D analysis. A 3-D analysis was performed on a localized area around the pin and the model also includes the rotor

[3]Unpublished data

hub lug. The 3-D model shown in figure 5 uses pentahedron and hexahedron elements of the EISI/EAL finite element code. The same symmetry conditions exist for the 3-D analysis and the 2-D analysis. Material properties used for the 3-D analysis are given in Table 3. Properties for the 1-2 directions are given in Table 2. Properties for the 3 direction were estimated since the values were not available in the literature.

To introduce a load in this model displacements were applied at Station 40.56. The displacement in the 3-D model, between the pin center (Sta 39.) and Station 40.56 were matched to the displacement in the 2-D Model between the pin center and Station 40.56.

DISCUSSION AND RESULTS

2-D Analysis

The results of the 2-D analysis for Boundary Condition II are shown in figures 6 thru 9. This boundary condition produced the highest stresses. Stress contours shown in figure 6 are for the complete model of Design (A) whereas the contours shown in figure 7 are for the spar caps (uni-directional Kevlar-49/epoxy) only. Each contour level indicates a line of constant stress. Stress values for each contour number are given in Table 4 and the far field stress was 57.4 MPa. The directions α and β are parallel and perpendicular respectively, to the uni-directional material in the spar caps. The dense concentration of σ_α stress contours in spar caps indicates a high stress gradient leading to the point of maximum stress. The σ_β and $\tau_{\alpha\beta}$ stress are very low (approximately 20% of σ_α). A plot of the stress concentrations across the attachment lug on a line thru the point of maximum stress is shown in figure 8 for Design (A). The stress concentrations equal the stress (σ_α) in the element divided by the far field stress (σ_0). The maximum stress concentration at the element adjacent to the pin is 5.92. The stress concentration for Design (B) is approximately the same as Design (A).

Radial stress in the uni-directional Kevlar-49/epoxy spar caps adjacent to the pin is shown in Figure 9 for Design (A) and boundary Condition II. The radial stress is 82 percent of the far field stress and the maximum value is also at the point of maximum circumferential stress concentration in the uni-directional fiber.

In order to assess the effect of potential manufacturing anomalies such as low fiber volume fraction, and voids, the elastic stiffness properties of the model for Design (A) were reduced 10 and 35 percent and the stress concentration factors were calculated. The reductions in elastic properties had less than 5 percent effect on the stress concentrations. These results indicate that the stress concentration factor is primarily a function of lug geometry for the range of material properties investigated. The axial stiffness of glass/epoxy is approximately 35 percent less than the value for Kevlar-49/epoxy. Based on the results of this study, stress concentrations in glass/epoxy or Kevlar-49/epoxy lugs would be approximately equal.

3-D Analysis

The stress contours plots for a plane that passes through the point of maximum stress are shown in figure 10 and for Design (A), Boundary Condition II. In the figure σ_θ is tangential to the pin and σ_r is in the radial direction. The Z-direction is through the lug thickness. Stress values for each contour are given in Table 5. The maximum stress concentration in the lug is 3.87. The point of maximum stress is located adjacent to the pin on the lower surface of the lug. The σ_r contours indicate the effect of the unidirectional fiber pulling against the pin, and the maximum value equals approximately 10 percent of σ_θ. The σ_z stresses result from Poisson contractions thru the thickness of the lug. The three shear stress components are shown in figure 11 and all values are less than 10 percent of σ_θ.

LUG DESIGN

The stress report for the initial design and analysis of the composite main rotor blade indicated that the following formula was used to compute the stress concentration factor:

$$K = \frac{1.3(R/r)^2 + 0.7}{(R/r) + 1.0} \tag{1}$$

where R is the lug outer radius and r is the lug inner radius. For Design (A), r = 1.8 cm, R = 3.57 cm and for Design (B), r = 1.8 cm, R = 3.66. Substituting into equation (1) gives K = 1.95 for Design (A) and 2.01 for Design (B). Based on the assumption that $E_l/E_t = 4$ and $\nu_{tl} = 0.075$, equation (1) was obtained by reducing the following equation:

$$K = \frac{(R/r)^2 + 1}{R/r + 1} + \frac{\nu_{tl}E_l}{E_t}\,\frac{(R/r)^2 - 1}{R/r + 1} \tag{2}$$

Equations (1) and (2) were obtained from reference 3. For the Kevlar-49/epoxy used in the present designs $E_l/E_t = 13.75$ and ν_{tl} is approximately 0.05. Substituting these values into equation (2) gives: K = 2.35. This stress concentration determined by equation (2) is less the one-half the value (5.92) determined by the 2-D analysis and two-thirds of the value (3.87) determined by the 3-D analysis.

COMPARISON OF ANALYSIS WITH PUBLISHED DATA

The computed stress concentration factors were compared with experimental data from the stress report and reference (5). Data from reference (4), for glass/epoxy lugs, are reproduced in figure (12), where lug efficiency factor E equals 1/K. Kevlar-49/epoxy data from the stress report is also included in figure 12. Four of the five Kevlar-49/epoxy data points are within the band width of the glass/epoxy data. The lug efficiency factors determined by the finite element analysis are 0.17 (2-D analysis) and 0.26 (3-D analysis) for the design referenced herein. These calculated points, shown in figure 12, are below the average experimental data and indicate that the efficiency of the designs referenced herein will be less than the designs reported in reference 4. Experimental data and equation (2) indicate that reducing the ratio of the outer radius to the inner radius, improves the lug efficiency by reducing the stress concentration factor.

CONCLUSIONS

The stress analysis of the root end of a composite main rotor blade for the AAH helicopter has been performed. The stress concentration factor determined by the finite element analysis is approximately twice the value used in the root end design. The analysis and test data indicate that the stress concentration factor is primarily a function of geometry for the range of the material properties investigated. Stress concentration in the lug can be reduced by decreasing the ratio of the lug outer radius to the inner radius.

REFERENCES

1. Whetstone, W. D.: SPAR Structural Analysis System Reference Manual NASA CR-145096-1, 1977.

2. EISI/SPAR Reference Manual, Program Execution; Engineering Information Systems Incorporated, San Jose, CA, January 1979.

3. Conen, H.: "Deformation und Versagen von GFK-Strangschlaufen", Kuhststoffr, 1944, p. 632-634.

4. Anderson R. G. and Covington, C. E.: "Composite Main Rotor Blade for the 214 Helicopter", 32nd Annual Forum AHS Preprint No. 1051, May 1976.

TABLE 1

CROSS SECTIONAL AREAS AND SKIN THICKNESS

STATION	SPAR AREA (cm^2)	SKIN THICKNESS (cm)
39.00	8.17	.36
40.75	8.17	.36
44.00	7.81	.36
48.50	7.3	.29
55.00	6.32	.16

TABLE 2

MATERIAL PROPERTIES FOR 2-D MODEL

	Kevlar-49/Epoxy	GR/Ep Tape	GR/Ep Fabric
E_l (GPa)	75.8	117.2	48.3
E_t (GPa)	5.5	11.7	48.3
G_{lt} (GPa)	2.1	5.9	6.9
ν_{lt}	.25	.25	.25

TABLE 3

MATERIAL PROPERTIES FOR 3-D ELEMENTS

Kevlar-49/Epoxy		
E_{11} = 75.8 GPa	G_{12} = 2.1 GPa	ν_{12} = .25
E_{22} = 5.5 GPa	G_{13} = 1.4 GPa	ν_{13} = .25
E_{33} = 5.5 GPa	G_{23} = 1.4 GPa	ν_{23} = .25

TABLE 4

STRESS CONTOUR VALUES FOR
2-D MODEL BOUNDARY CONDITION II
(REF. FIGURE 6 & 7)

STRESS COMPONENT	CONTOUR NUMBER	STRESS (MPa)
σ_{α}	1	0.
	2	25.
	3	50.
	4	75.
	5	100.
	6	125.
	7	150.
	8	175.
	9	200.
	10	225.
σ_{β}	1	-40.
	2	-35.
	3	-30.
	4	-25.
	5	-20.
	6	-15.
	7	-10.
	8	-5.
	9	0.
	10	5.
$\tau_{\alpha\beta}$	1	-50.
	2	-40.
	3	-30.
	4	-20.
	5	-10.
	6	0.
	7	10.
	8	20.
	9	30.
	10	40.

TABLE 5

STRESS CONTOUR VALUES FOR
3-D MODEL BOUNDARY CONDITION II
(REF. FIGURE 10 & 11)

STRESS COMPONENT	CONTOUR NUMBER	STRESS (MPa)
σ_θ	2	10.
	4	30.
	6	50.
	8	70.
	10	90.
	12	110.
	14	130.
	16	150.
	18	170.
	20	190.
σ_r	2	-22.
	4	-20.
	6	-18.
	8	-16.
	10	-14.
	12	-12.
	14	-10.
	16	-8.
	18	-6.
	20	-4.
σ_z	2	-1.85
	4	-1.55
	6	-1.25
	8	-.95
	10	-.65
	12	-.35
	14	-.05
	16	.25
	18	.55
	20	.85

TABLE 5

(CONTINUED)

STRESS COMPONENT	CONTOUR NUMBER	STRESS (MPa)
$\tau_{r\theta}$	2	1.
	4	3.
	6	5.
	8	7.
	10	9.
	12	11.
	14	13.
	16	15.
	18	17.
	20	19.
τ_{rz}	2	-1.5
	4	-3.5
	6	-5.5
	8	-7.5
	10	-9.5
	12	-11.5
	14	-13.5
	16	-15.5
	18	-17.5
	20	-19.5
$\tau_{z\theta}$	2	-4.
	4	-2.
	6	0.
	8	2.
	10	4.
	12	6.
	14	8.
	16	10.
	18	12.
	20	14.

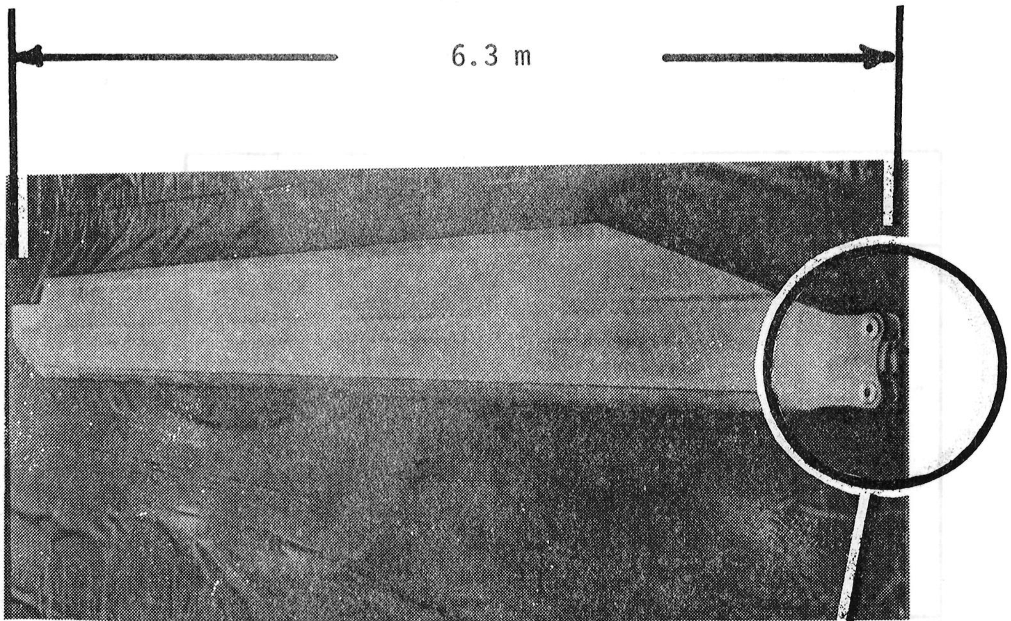

a) Complete Blade

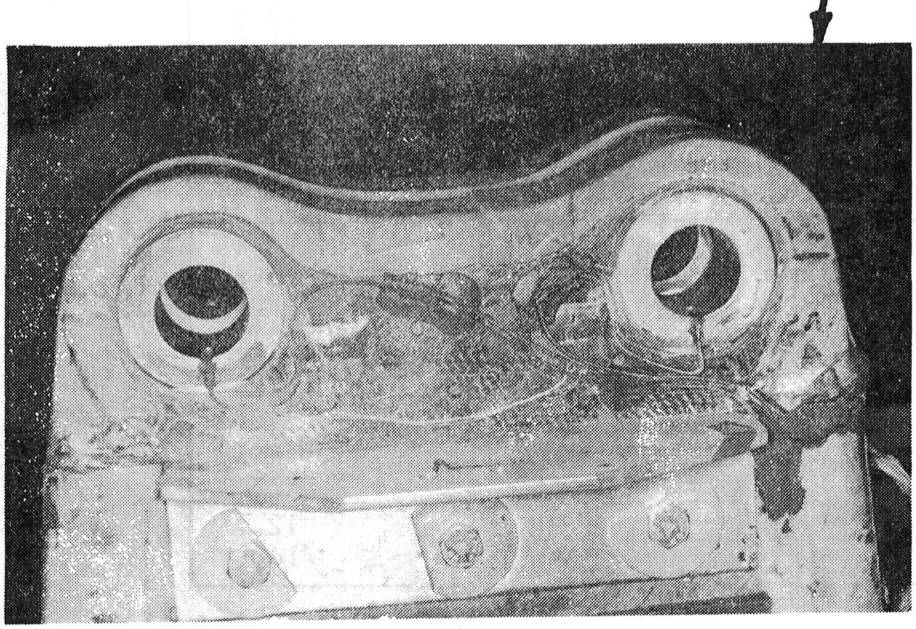

b) Root End (Rotated View)

Figure 1 - AAH Composite Main Rotor Blade

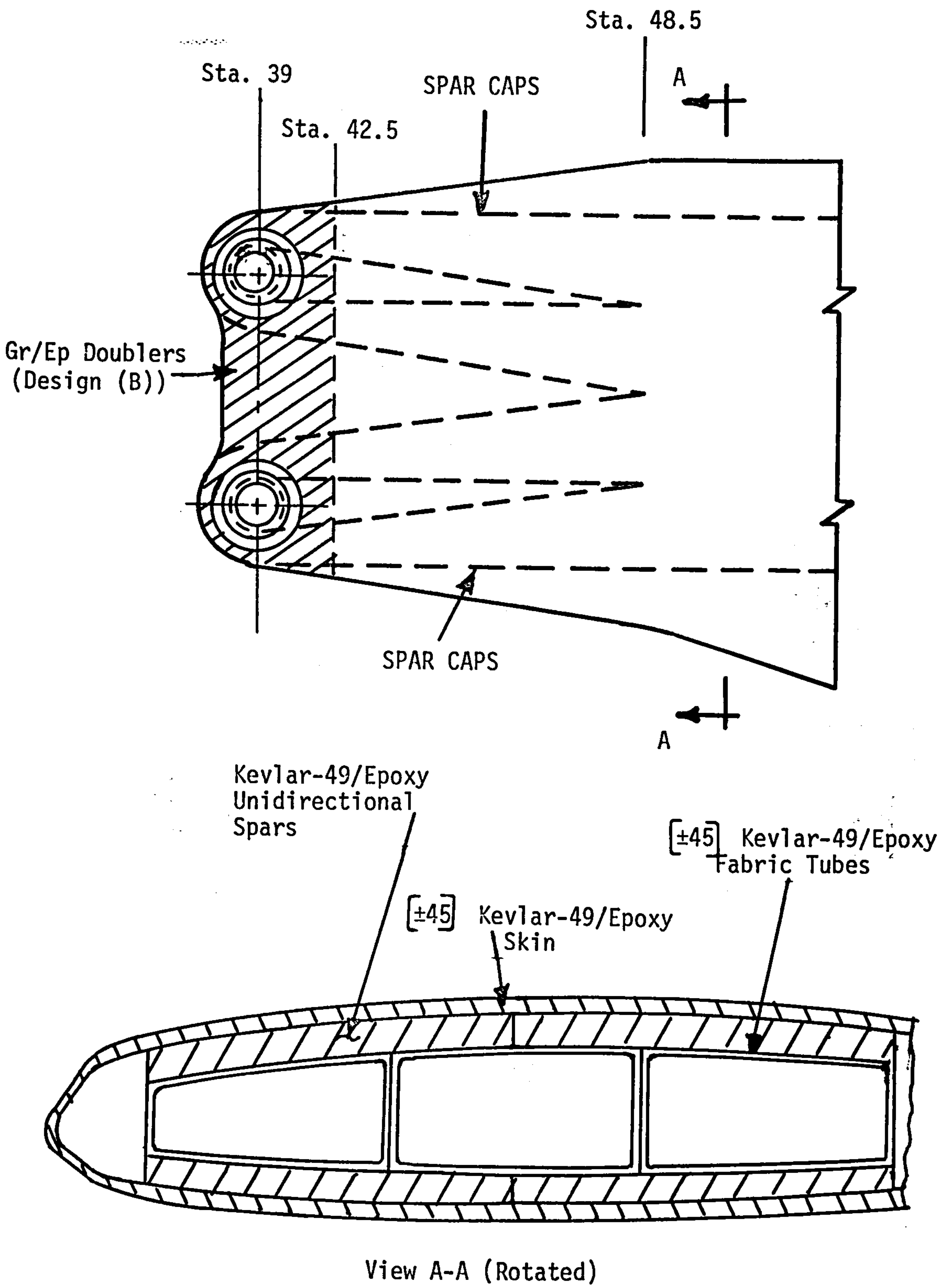

Figure 2. - Root-end of blade

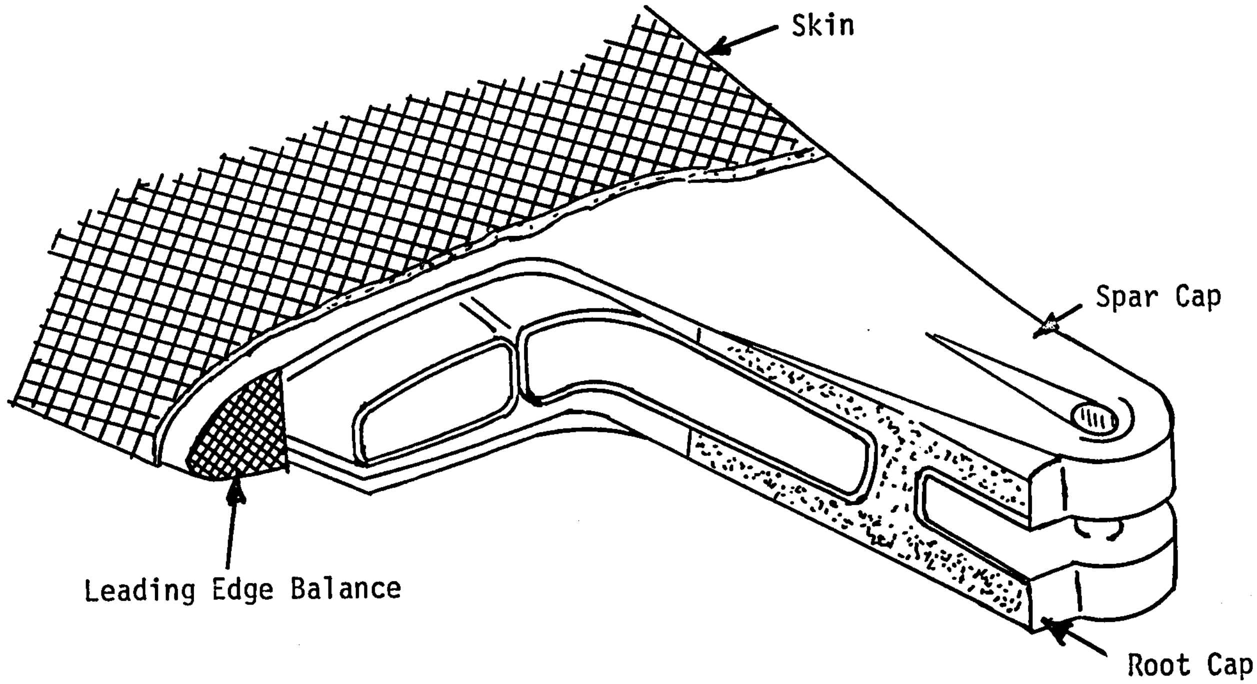

Figure 3 - Isometric view of the root end of composite main rotor blade

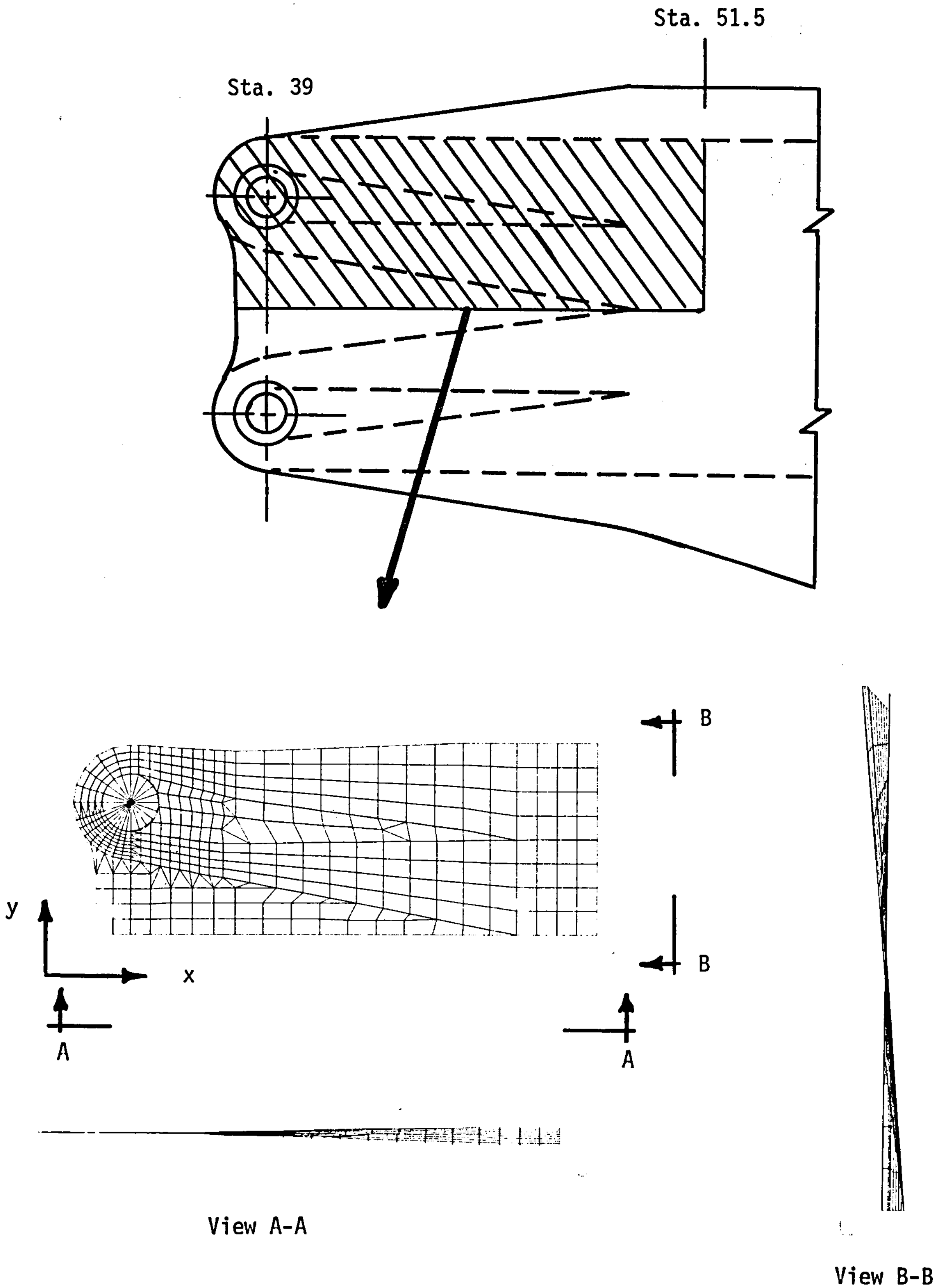

Figure 4 - 2-D Finite Element Model

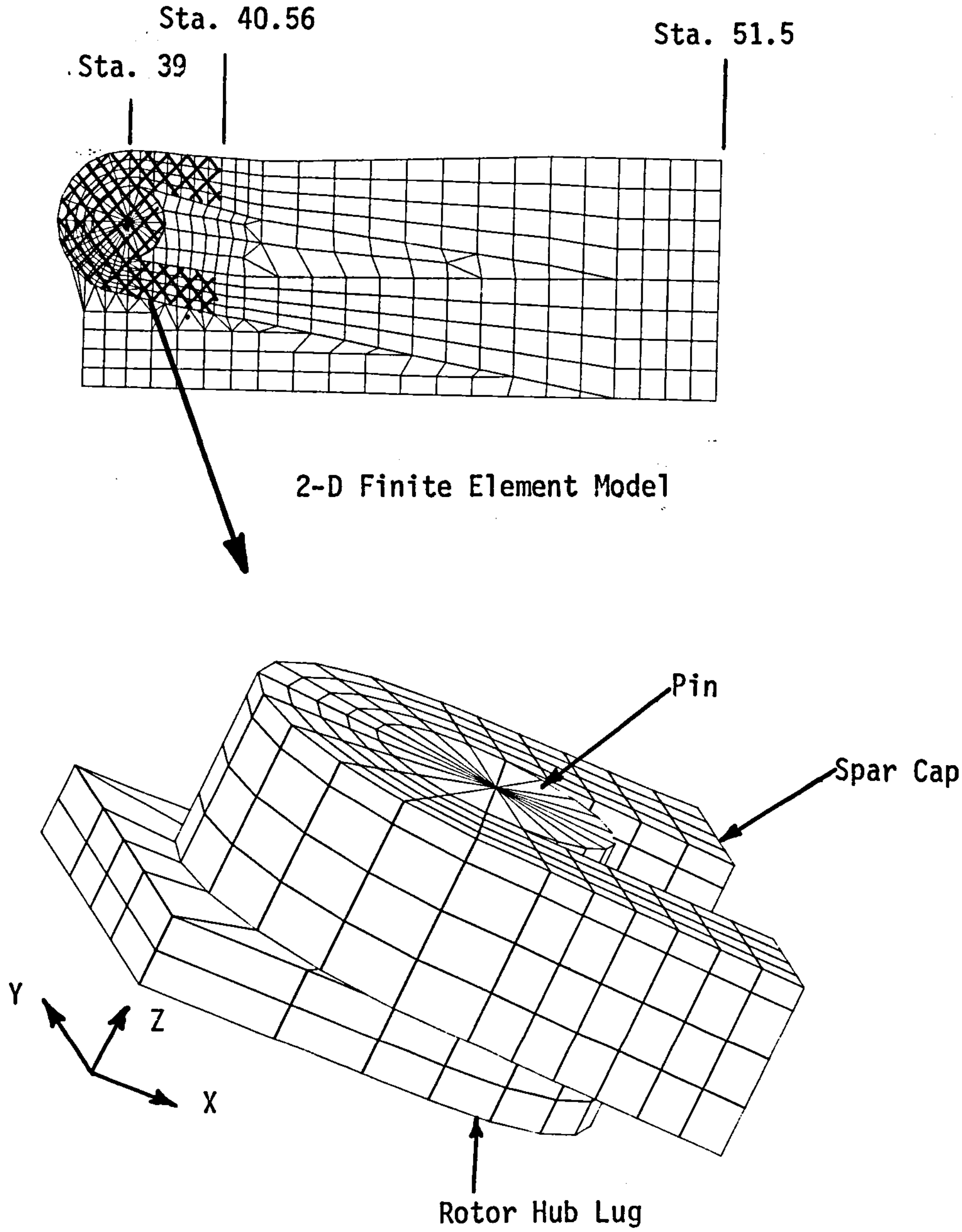

Figure 5 - 3-D Finite Element Model

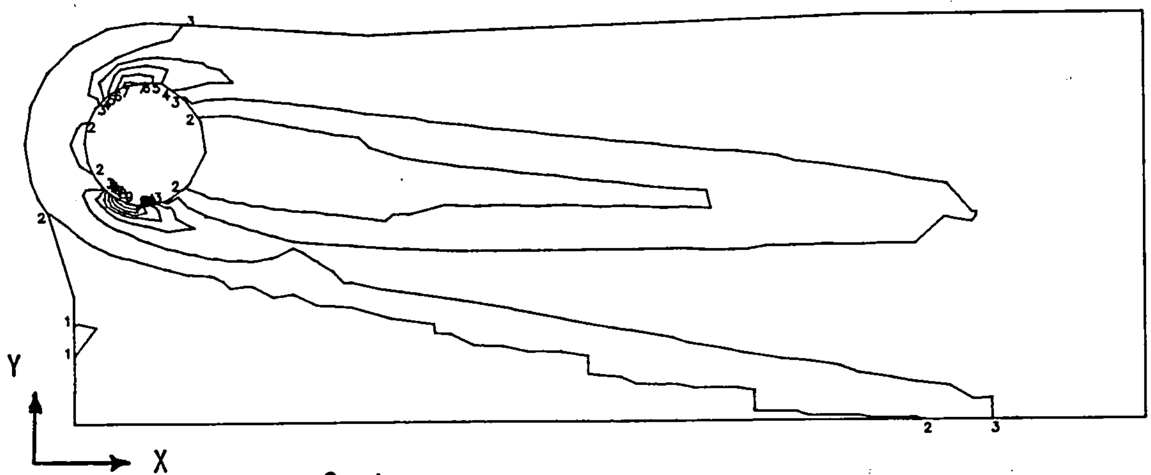

σ_{α} Contours

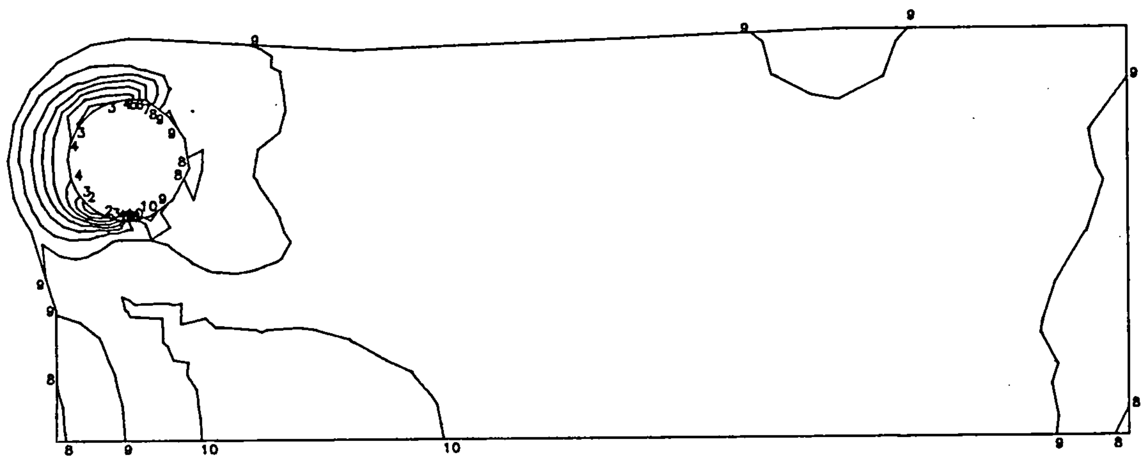

σ_{β} Contours

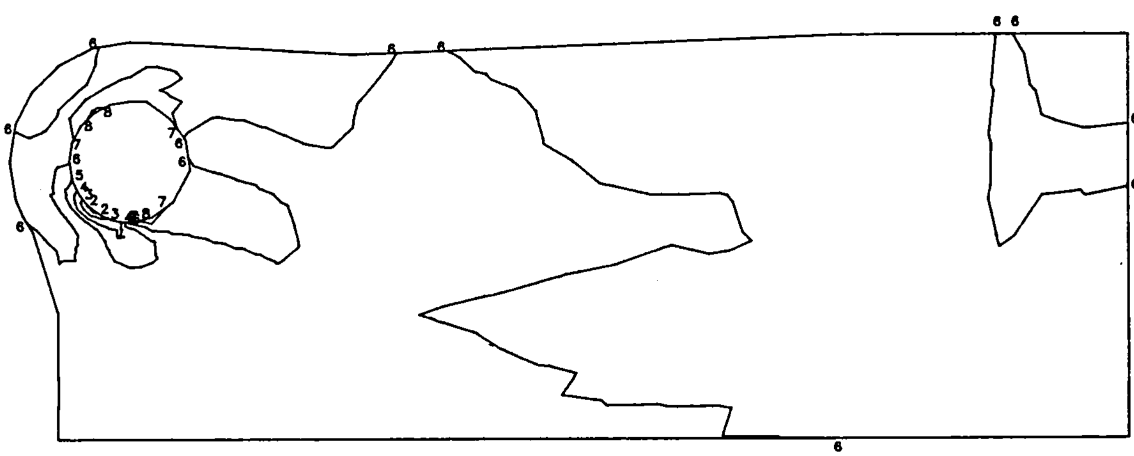

$\tau_{\alpha\beta}$ Contours

Figure 6- Stress Contours for Complete Model of Design (A), Boundary Condition II.

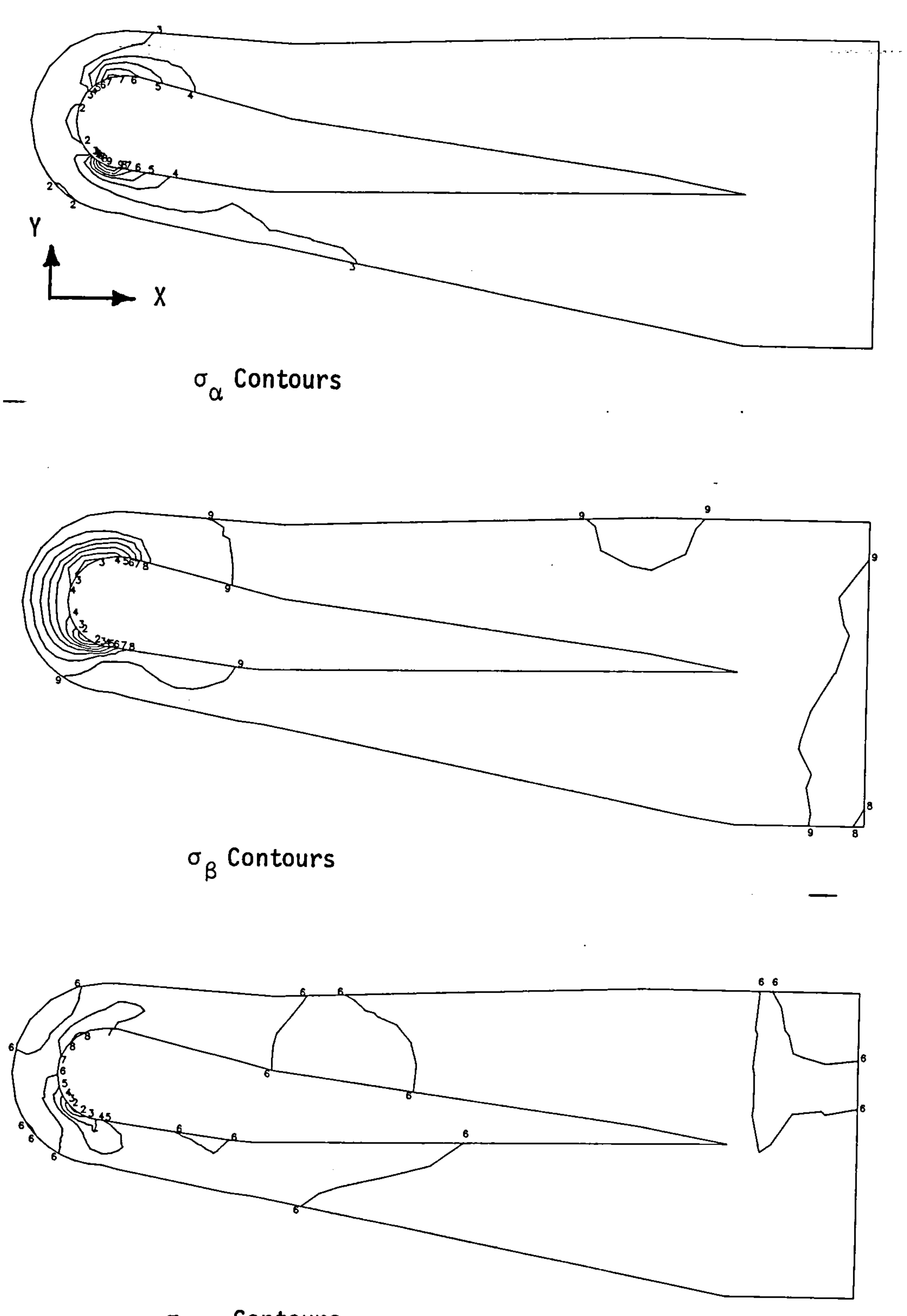

Figure 7- Stress Contours in Spar Caps of Design (A).

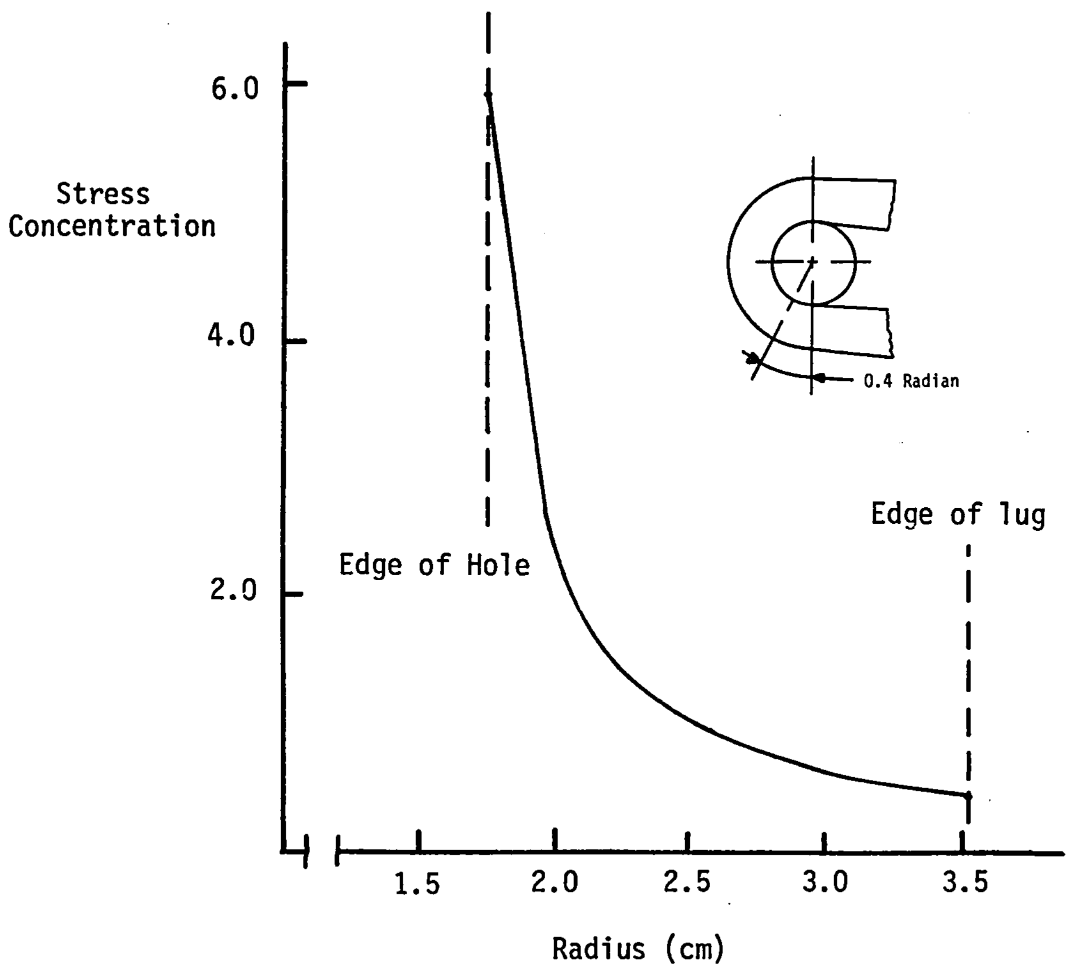

Figure 8 - Stress Concentration in Lug on a Line
Thru Point of Maximum Stress for Design (A).

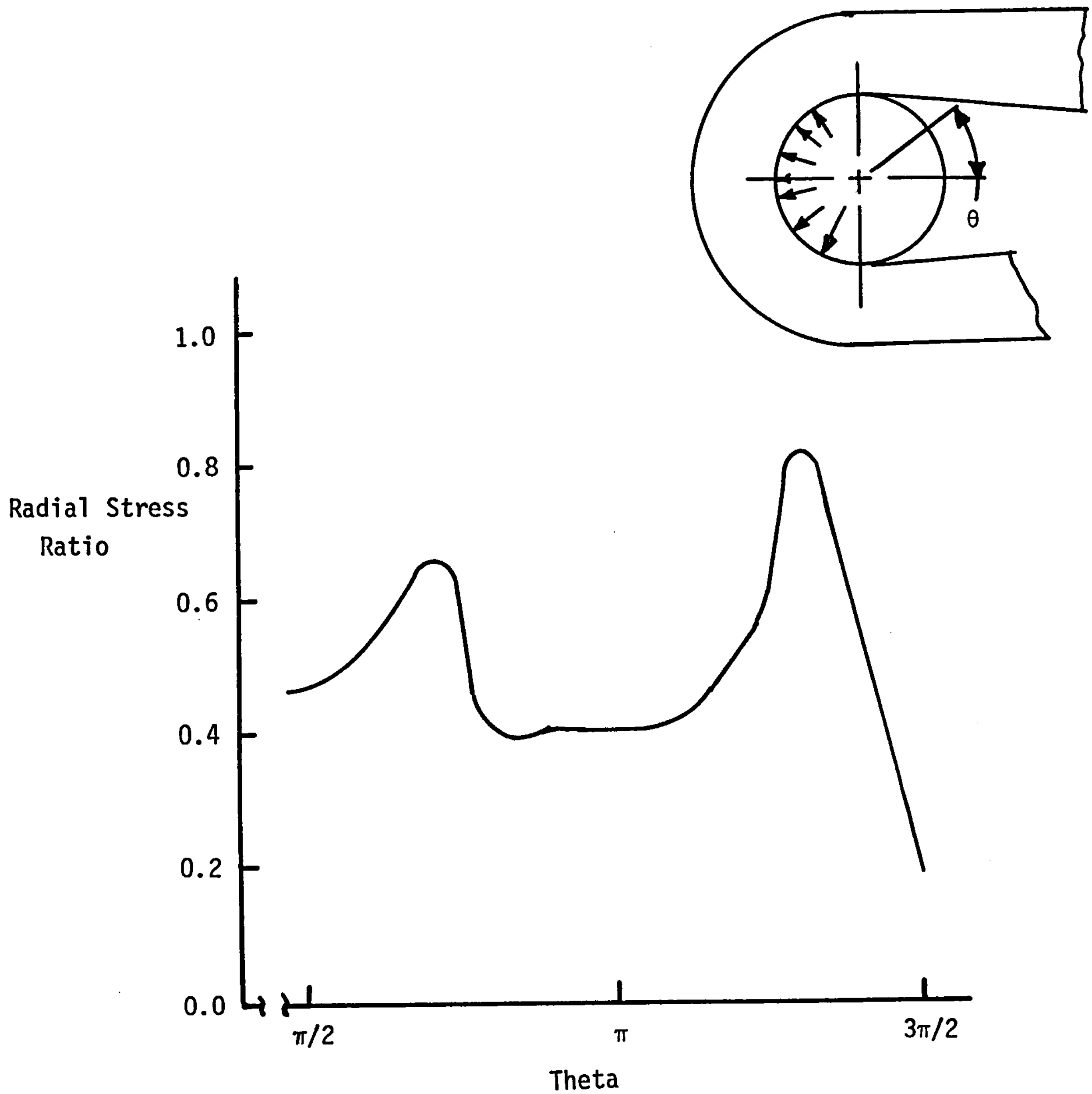

Figure 9- Radial Stress in Lug Adjacent to Pin, for Design (A).

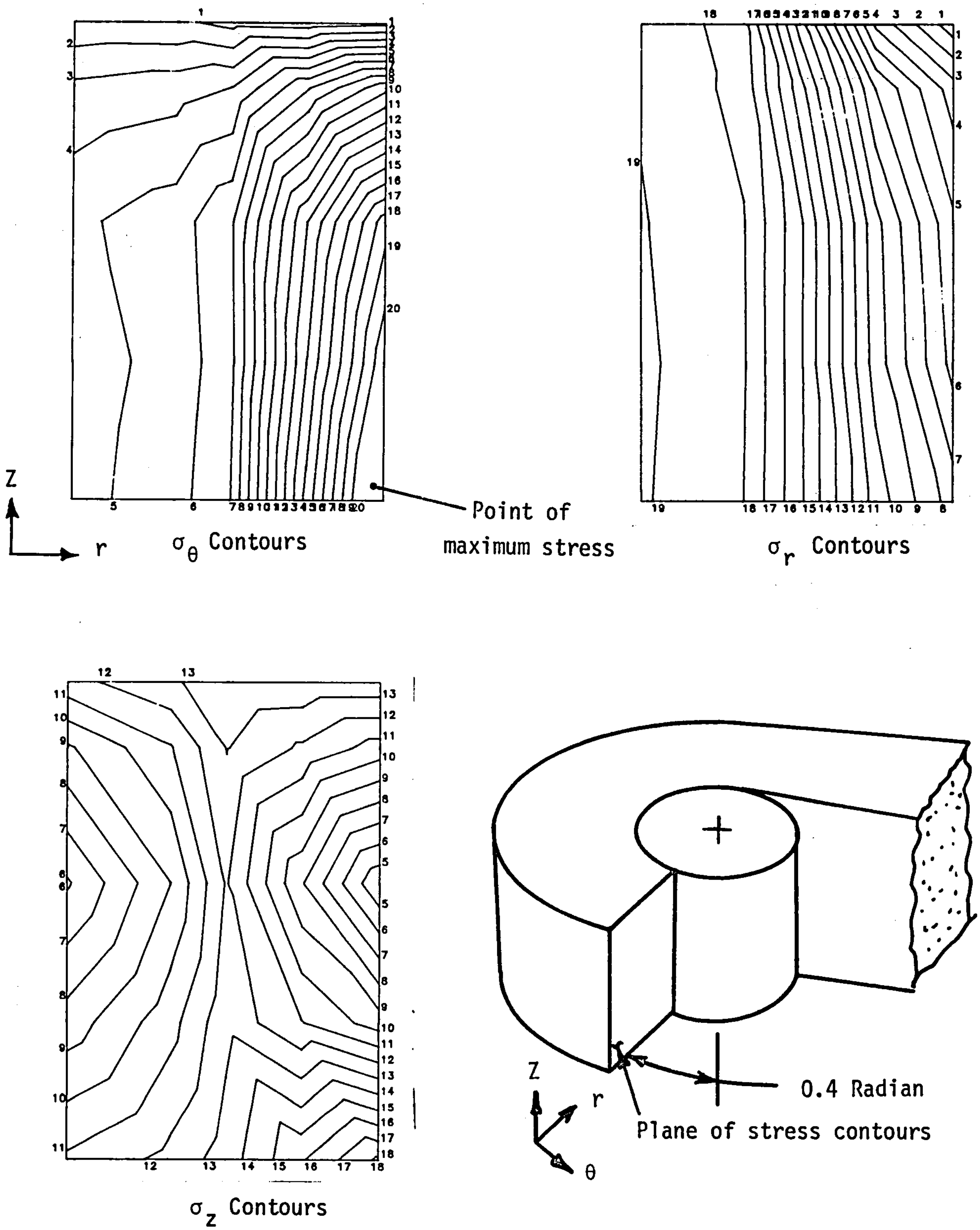

Figure 10- Noraml Stress Contours From 3-D Analysis for Design (A), Boundary Condition II.

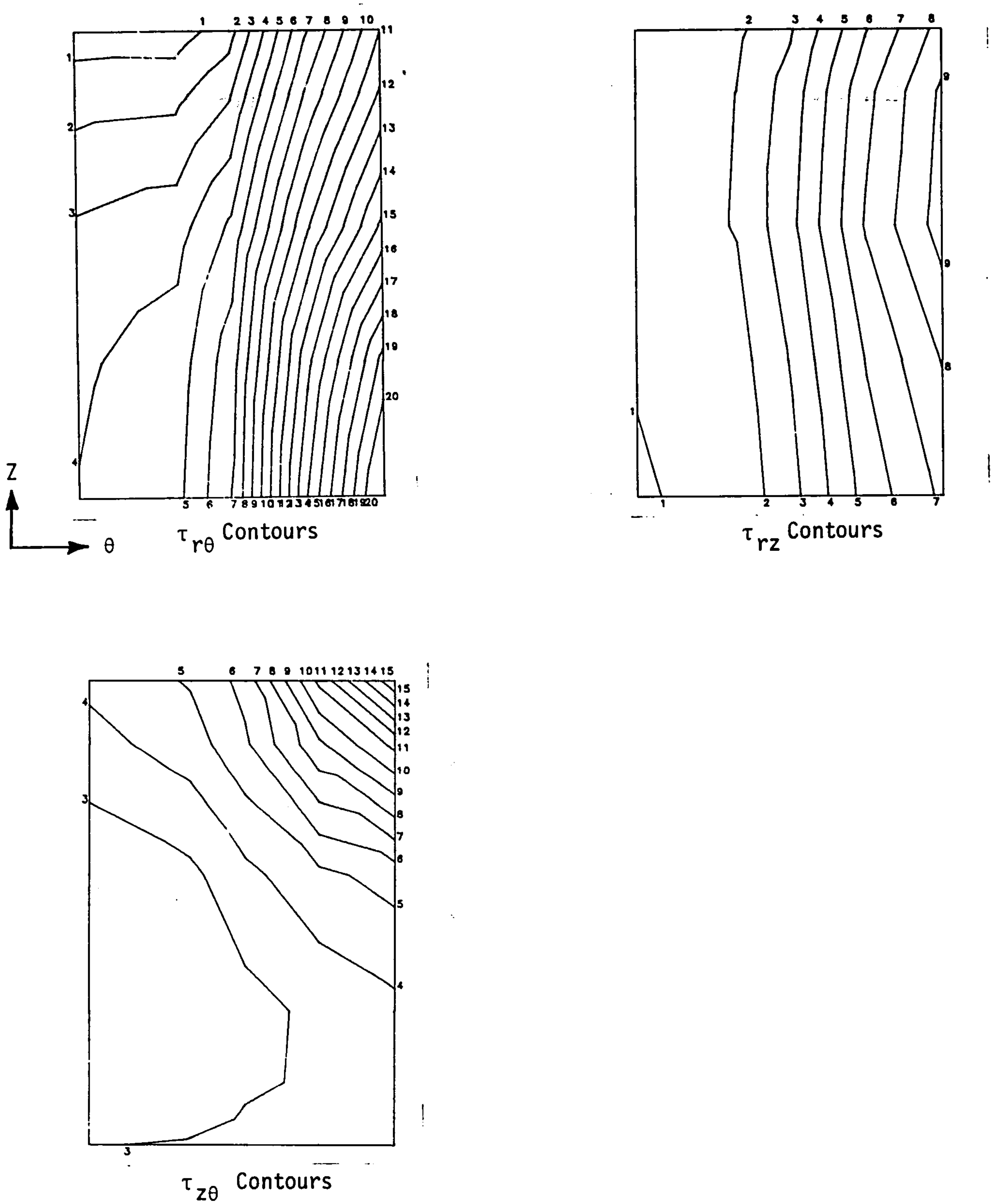

Figure 11- Shear Stress Contours From 3-D Analysis for Design (A), Boundary Condtion II.

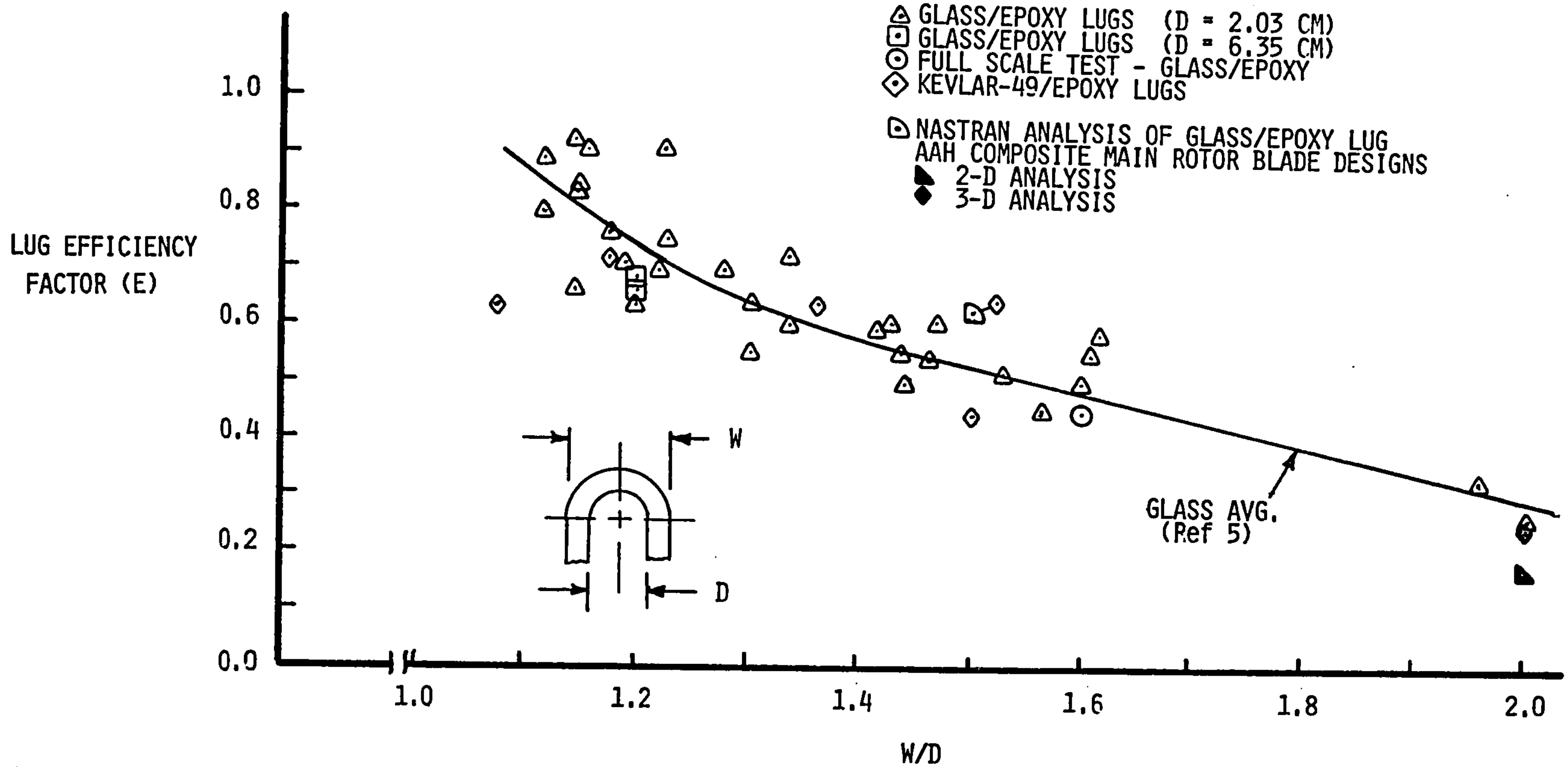

FIGURE 12. - LUG EFFICIENCY FACTOR

1. Report No.	2. Government Accession No.	3. Recipient's Catalog No.
NASA TM-84578		

4. Title and Subtitle	
STRESS ANALYSIS OF ADVANCED ATTACK HELICOPTER COMPOSITE MAIN ROTOR BLADE ROOT END LUG	5. Report Date December 1982
	6. Performing Organization Code 532-06-13-01
7. Author(s) Donald J. Baker	8. Performing Organization Report No.
9. Performing Organization Name and Address NASA Langley Research Center Hampton, VA 23665	10. Work Unit No.
	11. Contract or Grant No.
12. Sponsoring Agency Name and Address National Aeronautics and Space Administration Washington, DC 20546	13. Type of Report and Period Covered Technical Memorandum
	14. Sponsoring Agency Code

15. Supplementary Notes

The author is employed by the Structures Laboratory,USARTL (AVRADCOM)

16. Abstract

Stress analysis of the Advanced Attack Helicopter (AAH) composite main rotor blade root end lug is described. The stress concentration factor determined from a finite element analysis is compared to an empirical value used in the lug design. The analysis and test data indicate that the stress concentration is primarily a function of configuration and independent of the range of material properties typical of Kevlar-49/Epoxy and Glass/Epoxy.

17. Key Words (Suggested by Author(s))	18. Distribution Statement
Composite Materials Rotor Blade Stress Analysis	Unclassified - Unlimited Subject Category - 24

19. Security Classif. (of this report)	20. Security Classif. (of this page)	21. No. of Pages	22. Price*
Unclassified	Unclassified	24	A02

N-305

For sale by the National Technical Information Service, Springfield, Virginia 22161